

An extinction analysis for rotating-disk flame under low pressures

Peng Zhang* and Chung K. Law

*Department of Mechanical and Aerospace Engineering, Princeton University
Princeton, New Jersey 08544, USA*

Abstract

An asymptotic theory based on the large activation energy assumption of one-step overall gas-phase reaction was formulated for the extinction of a premixed rotating-disk flame under low pressure which renders the flow weakly rarefied. A similarity solution was obtained for such a flow so that the theory can be unified with previous theories of flame extinction in stagnation and boundary layer flows. Extinction criteria based on the critical Damköhler number were obtained through the S-curve concept to elucidate the effects of the CVD operating conditions that flame extinction is delayed with decreasing the spin rate of the disk and/or increasing the disk temperature. Furthermore, while decreasing pressure and therefore the reactivity of the mixture tends to extinguish the flame, the trend can be substantially weakened by taking into account of the influence of the Knudsen layer, which renders flame extinction harder by reducing the heat loss to the cold disk and the flow stretch rate at the flame.

1. Introduction

Flame-assisted chemical vapor deposition (FACVD) has been widely used for material synthesis (e.g. Komaki 1993; Kim & Cappelli 1994; Glumac & Goodwin 1996; Goodwin, Glumac & Shin 1996). In such a reactor, say for the deposition of diamond films, a premixed flame is stabilized over a heated substrate impinged by a fuel-rich ethylene-oxygen mixture flow, within which the reaction products from the flame are brought toward and subsequently deposited on the substrate through surface reactions. In order to obtain desirable properties of the film, studies have been conducted to identify optimum operating conditions of FACVD, such as the fuel type, the equivalence ratio, the substrate temperature, the flow type and the system pressure. For example, it was experimentally observed that large area coverage and high uniformity of the diamond deposition can be achieved by reducing the system pressure and/or spinning the substrate to stretch the flame (e.g. Tzeng 1991). Since the operation of FACVD requires a steady flame, which however could be extinguished by increasing the spin rate of the rotating substrate and/or decreasing the system pressure, an analysis yielding the parametric influence on the state of flame extinction is of obvious practical interest.

The problem that we shall analyze is as follows: an infinite disk rotates about its symmetry axis in a stationary fluid composed of a chemically reacting premixture. The fluid near the disk is thrown outwardly by the viscosity and a compensating flow is accordingly induced to impinge the disk. Due to the self-similarity of the rotating-disk flow (e.g. Kármán 1921, Schlichting 1968), the axial velocity, temperature and species concentration only depend on the axial distance from the disk, and a flat rotating flame can be stabilized over the disk. Consequently, such a flow configuration has advantages in synthesizing deposition films with high uniformity and large area coverage. It is noted that, while the self-similar characteristics of the rotating-disk flow exists only for a disk with infinite radius, it is also a good approximation for a finite disk over a large fraction of the radial direction when the spin rate of the rotating disk is sufficiently large (Coltrin, Kee & Evans 1989; Kee, Coltrin & Glarborg 2003).

Low-pressure FACVD has been experimentally demonstrated to be able to further promote the uniformity and area coverage of diamond film deposition with a reduced growth rate, because reducing the operation pressure tends to improve the purity of deposition film by restraining unwanted gas-phase reactions and enhance the controllability of the substrate temperature (e.g. Goodwin, Glumac & Shin 1996). However, in the prevalent pressure range, rarefied gas effects

*Corresponding author: pengz@princeton.edu
Proceedings of the 6th U.S. National Combustion Meeting

could be important and as such need to be considered in the analysis. Mechanistically, we recognize that the rotating-disk flow has a boundary-layer-like flow structure, whose characteristic length is about 1.0mm in atmospheric pressure for characteristic spin rates of 1000 rpm, and is inversely proportional to the square root of the pressure, while the mean free path of the gas mixture is about 10^{-4} mm in one atmosphere and is inversely proportional to the pressure. As a consequence of decreasing the pressure, the Knudsen number, Kn , which is a measure of the gas rarefaction and is defined as the ratio of the mean free path to the characteristic length, could be in the range of $O(10^{-3} - 10^{-1})$ in the prevalent operating conditions of FACVD, and as such renders the flow to be weakly rarefied. Physically, the weakly rarefied rotating-disk flow consists of a continuum boundary-layer flow with the Knudsen layer next to the disk, in which the distribution function of gas molecules is generally non-Maxwellian, or non-equilibrium, and the continuum description is not valid. To account for effects of the Knudsen layer, weakly rarefied flows are conventionally studied in the framework of the continuum mechanics but with appropriate slip boundary conditions (e.g. Kogan 1969), indicating the concept that the physical properties (e.g. velocity, temperature and concentration) of the flow at the disk, as perceived by the flow, are not the same as those of the disk but instead possess a certain amount of slip. It is expected that the presence of slip properties will change the flow field and hence influence the flame extinction.

Asymptotic analysis of flame extinction based on the large activation energy assumption of a one-step overall reaction is well established in combustion theory and has been performed for stagnation and boundary layer flows (e.g. Chung, Kim & Law 1986; Chung 1988; Law 2006). Consequently, the present analysis can be considered as an extension of the existing theories to rotating-disk flows and will be performed following the standard procedure. Through such an analysis, information about the extinction characteristics of a reactive system can be obtained by analyzing the S-curve, which describes the response of the flame intensity to the Damköler number, Da , defined as the ratio of the characteristic flow time to the characteristic reaction time. A steady flame cannot be sustained when Da becomes smaller than a critical value - the extinction Damköler number, which is identified as the turning point of the upper-half of the S-curve. Thus, the major objective of the present study is to obtain the S-curve of the rotating-disk flame, identify the corresponding extinction Damköler number, and elucidate their dependence on the flow conditions, especially on the pressure.

Formulation of the present problem will be presented in the next section, followed by the extinction analysis and results in §3.

2. Formulation

2.1. Governing equations

We consider a steady axisymmetric rotating-disk flow for a chemically reacting premixture with variable properties. A cylindrical coordinate system (r, ϕ, z) is so established that the disk is located on the plane $z = 0$ and rotates about the z -axis with an angular velocity Ω ; the flow velocity components are denoted by (u, v, w) corresponding to (r, ϕ, z) , respectively. The governing equations for the flow are given by the continuity equation,

$$\frac{1}{r} \frac{\partial}{\partial r}(r\rho u) + \frac{\partial}{\partial z}(\rho w) = 0, \quad (1)$$

the radial momentum equation,

$$\begin{aligned} \rho \left(u \frac{\partial u}{\partial r} + w \frac{\partial u}{\partial z} - \frac{v^2}{r} \right) &= -\frac{\partial p}{\partial r} \\ + \frac{\partial}{\partial r} \left\{ 2\mu \frac{\partial u}{\partial r} - \frac{2}{3}\mu \left[\frac{1}{r} \frac{\partial}{\partial r}(ru) + \frac{\partial w}{\partial z} \right] \right\} \\ + \frac{\partial}{\partial z} \left[\mu \left(\frac{\partial u}{\partial z} + \frac{\partial w}{\partial r} \right) \right] &+ \frac{2u}{r} \left(\frac{\partial u}{\partial r} - \frac{u}{r} \right), \end{aligned} \quad (2)$$

the circumferential momentum equation,

$$\begin{aligned} \rho \left(u \frac{\partial v}{\partial r} + w \frac{\partial v}{\partial z} + \frac{uv}{r} \right) &= \frac{\partial}{\partial r} \left[\mu \left(\frac{\partial v}{\partial r} - \frac{v}{r} \right) \right] \\ + \frac{\partial}{\partial z} \left[\mu \left(\frac{\partial v}{\partial z} \right) \right] &+ \frac{2u}{r} \left(\frac{\partial v}{\partial r} - \frac{v}{r} \right), \end{aligned} \quad (3)$$

the axial momentum equation,

$$\begin{aligned} \rho \left(u \frac{\partial w}{\partial r} + w \frac{\partial w}{\partial z} \right) &= -\frac{\partial p}{\partial z} \\ + \frac{\partial}{\partial z} \left\{ 2\mu \frac{\partial w}{\partial z} - \frac{2}{3}\mu \left[\frac{1}{r} \frac{\partial}{\partial r}(ru) + \frac{\partial w}{\partial z} \right] \right\} \\ + \frac{1}{r} \frac{\partial}{\partial r} \left[\mu r \left(\frac{\partial u}{\partial z} + \frac{\partial w}{\partial r} \right) \right], \end{aligned} \quad (4)$$

the species equation,

$$\begin{aligned} \rho \left(u \frac{\partial Y}{\partial r} + w \frac{\partial Y}{\partial z} \right) \\ - \left[\frac{\partial}{\partial r} \left(\rho D \frac{\partial Y}{\partial r} \right) + \rho D \frac{1}{r} \frac{\partial Y}{\partial r} + \frac{\partial}{\partial z} \left(\rho D \frac{\partial Y}{\partial z} \right) \right] \\ = -\omega, \end{aligned} \quad (5)$$

the energy equation,

$$\begin{aligned} & \rho c_p \left(u \frac{\partial T}{\partial r} + w \frac{\partial T}{\partial z} \right) \\ & - \left[\frac{\partial}{\partial r} \left(\lambda \frac{\partial T}{\partial r} \right) + \lambda \frac{1}{r} \frac{\partial T}{\partial r} + \frac{\partial}{\partial z} \left(\lambda \frac{\partial T}{\partial z} \right) \right] \\ & = q_c \omega, \end{aligned} \quad (6)$$

and the ideal gas law,

$$p = \rho R^o T / \bar{W}, \quad (7)$$

where ρ is the density, p the pressure, T the temperature, μ the viscosity, D the mass diffusivity, λ the thermal diffusivity, and R^o the universal gas constant. The average molecular weight of the mixture \bar{W} , the specific heat capacity c_p and the heat of combustion q_c are assumed to be constants. In deriving (5) and (6), we have assumed that the mixture is sufficiently off-stoichiometric that the reaction is governed by the mass fraction Y of the deficient reactant, which corresponds to the oxidizer in the fuel-rich hydrocarbon-oxygen mixture, and hence a one-reactant, one-step overall reaction, Reactant \rightarrow Products, is used in the present formulation. Consequently, the reaction rate ω can be expressed by $\omega = B \rho^n Y e^{-E_a/R^o T}$, where the overall reaction order n is close to 2 at low pressures; the activation energy E_a and the collision rate factor B can be treated as constants. It is noted that we have neglected the expansion work by the pressure and the viscous dissipation in (6) since they are negligibly small compared to the chemical heat release.

Equations (1)-(7) are to be solved subject to the boundary conditions at infinity,

$$u = v = 0; \quad T = T_\infty; \quad Y = Y_\infty, \quad (8)$$

where the subscript ∞ denotes the physical quantities at $z = \infty$, and the slip boundary conditions at the disk (Shidlovskiy 1967, Gupta 1985),

$$u = \frac{2 - \alpha_V}{\alpha_V} l_m \frac{\partial u}{\partial z}, \quad v = \Omega r + \frac{2 - \alpha_V}{\alpha_V} l_m \frac{\partial v}{\partial z}, \quad w = 0, \quad (9)$$

$$T = T_w + \frac{2 - \alpha_T}{\alpha_T} \frac{2\gamma}{1 + \gamma} \frac{1}{Pr} l_m \frac{\partial T}{\partial z}; \quad \frac{\partial Y}{\partial z} = 0, \quad (10)$$

where l_m is the mean free path of gas molecules, α_V the accommodation coefficient for velocity, α_T the accommodation coefficient for temperature, γ the heat capacity ratio, and Pr the Prandtl number. In deriving (9) and (10), we have neglected the chemical deposition of gas species at the disk since the deposition rate is usually so small that the induced axial velocity at the disk surface and the concomitant heat release have negligible influence on the flow.

2.2. Similarity formulation

Following the approach of von Kármán (1921) and Ostrach & Thornton (1958), we seek a similarity solution of (1)-(7) in the form

$$\begin{aligned} u(r, z) &= \Omega r F(\zeta), \\ v(r, z) &= \Omega r G(\zeta), \\ w(r, z) &= (\rho_\infty / \rho) \sqrt{\Omega \nu_\infty} H(\zeta); \\ T(r, z) &= (Y_\infty q_c / c_p) \tilde{T}(\zeta); \\ Y(r, z) &= Y_\infty \tilde{Y}(\zeta); \\ p(r, z) &= \rho_\infty \nu_\infty \Omega P(\zeta), \end{aligned} \quad (11)$$

where $\zeta = \sqrt{\Omega / \nu_\infty} \int_0^z \rho(\eta) / \rho_\infty d\eta$ is a nondimensional coordinate and $\nu = \mu / \rho$ the kinematic viscosity. Noting that the pressure variation along the z -axis has been shown to be of the order of $O(\rho_\infty \nu_\infty \Omega)$ (e.g. Cochran 1934), which is much smaller than the inflow pressure p_∞ of interest, we can therefore neglect the pressure variation in the axial direction by replacing (4) by $\partial p / \partial z = 0$. Furthermore, we assume that $\mu(z)$ obeys the linear viscosity-temperature law $\mu(z) / T(z) = \mu_\infty / T_\infty$, which, together with the constant pressure assumption, results in the Chapman-Rubeson assumption $\rho(z) \mu(z) = \rho_\infty \mu_\infty$. Furthermore, $D(z)$ and $\lambda(z)$ are assumed to vary in the way that the Schmidt number $Sc = \mu / \rho D$ and the Prandtl number $Pr = \mu c_p / \lambda$ are constant.

Substituting (11) and (12) into the governing equations (1)-(6) and the boundary conditions (8)-(10), we have the following ODE system:

$$2F + H' = 0, \quad (13)$$

$$F^2 + HF' - G^2 = F'', \quad (14)$$

$$2FG + HG' = G'', \quad (15)$$

$$P' = 0, \quad (16)$$

$$H\tilde{Y}' - \tilde{Y}'' / Sc = -\omega / \rho Y_\infty \Omega, \quad (17)$$

$$H\tilde{T}' - \tilde{T}'' / Pr = \omega / \rho Y_\infty \Omega, \quad (18)$$

which are subject to the boundary conditions at $\zeta = \infty$,

$$F = G = 0; \quad \tilde{T} = \tilde{T}_\infty; \quad \tilde{Y} = 1, \quad (19)$$

and the slip boundary conditions at $\zeta = 0$,

$$F = Kn_V F', \quad H = 0, \quad G = 1 + Kn_V G', \quad (20)$$

$$\tilde{T} = \tilde{T}_w + Kn_T \tilde{T}'; \quad \tilde{Y}' = 0, \quad (21)$$

where the superscript prime represents derivatives with respect to the coordinate ζ ; $\tilde{T}_\infty = T_\infty c_p / Y_\infty q_c$ and

$\tilde{T}_w = T_w c_p / Y_\infty q_c$; the Knudsen number Kn_V and Kn_T are defined by

$$\begin{aligned} Kn_V &= l_m \frac{2 - \alpha_V}{\alpha_V} \left(\frac{\Omega}{v_\infty} \right)^{1/2} \frac{\rho}{\rho_\infty}, \\ Kn_T &= l_m \frac{2 - \alpha_T}{\alpha_T} \frac{2\gamma}{1 + \gamma} \frac{1}{Pr} \left(\frac{\Omega}{v_\infty} \right)^{1/2} \frac{\rho}{\rho_\infty}, \end{aligned} \quad (22)$$

which are considered to satisfy $O(Kn_V) = O(Kn_S) \ll 1$ in the present study.

2.3. Series solution

To solve the ODE system derived in §2.2, we first note that (13)-(15) subject to (19) and (20) can be solved independently from (17) and (18). The series solutions up to $O(Kn)$ is given by (Shidlovskiy 1967)

$$\begin{aligned} F &= F_0 + Kn_V F'_0, \\ G &= G_0 + Kn_V G'_0, \\ H &= H_0 + Kn_V H'_0, \end{aligned} \quad (23)$$

where the leading-order solutions F_0 , G_0 and H_0 satisfy (13)-(15) subject to

$$\begin{aligned} F_0(0) &= G_0(0) = 0; \\ F_0(\infty) &= 0, G_0(\infty) = 1, H_0(\infty) = 0. \end{aligned} \quad (24)$$

Noting that (13)-(15) and (24) are exactly the same equations derived by von Kármán (1921) for an incompressible rotating disk flow with constant properties, we can hence use the corresponding series solutions given by Cochran (1934):

$$\begin{aligned} H_0(\zeta \leq \zeta_0) &= -a\zeta^2 + \zeta^3/3 + b\zeta^4/6 + b^2\zeta^5/30 + a\zeta^6/180, \\ H_0(\zeta > \zeta_0) &= -c + \frac{2A}{c} e^{-c\zeta} - \frac{A^2 + B^2}{2c^3} e^{-2c\zeta} + \frac{A(A^2 + B^2)}{6c^5} e^{-3c\zeta} \\ &\quad - \frac{(A^2 + B^2)(17A^2 + B^2)}{288c^7} e^{-4c\zeta}, \end{aligned} \quad (25)$$

where $a = 0.510$, $b = -0.616$, $c = 0.886$, $A = 0.934$ and $B = 1.208$; $\zeta_0 = 0.9828$ is determined by matching the asymptotic solutions at a point where H_0 is continuous.

By further introducing a new flow-related coordinate (e.g. Law 2006)

$$\begin{aligned} \xi &= S(\zeta)/S(\infty), \\ S(\zeta) &= \int_0^\zeta \exp \left\{ \int_0^{\zeta'} H(\zeta'') d\zeta'' \right\} d\zeta', \end{aligned} \quad (26)$$

and assuming $Sc = Pr = 1$, we can rewrite (17)-(19) and (21) as

$$\frac{d^2}{d\xi^2} (\tilde{T} + \tilde{Y}) = 0, \quad (27)$$

$$\frac{d^2 \tilde{T}}{d\xi^2} = - \left[\frac{S(\infty)}{S'(\zeta)} \right]^2 Da \tilde{Y} e^{-\tilde{T}_a/\tilde{T}}, \quad (28)$$

$$\xi = 1 : \tilde{T} = \tilde{T}_\infty; \tilde{Y} = 1, \quad (29)$$

$$\xi = 0 : \tilde{T} = \tilde{T}_w + Kn_S d\tilde{T}/d\xi; d\tilde{Y}/d\xi = 0, \quad (30)$$

where $Da = B\rho^{n-1}/\Omega$ is the Damköhler number, which represents the ratio of the characteristic flow time to the characteristic reaction time, $Kn_S = S'(0)/S(\infty)Kn_T$ the flow-modified Kn_T , and $\tilde{T}_a = E_a c_p / R^0 Y_\infty q_c$ the nondimensional activation energy.

Equation (27) can be readily solved, yielding

$$\tilde{Y} = 1 + \tilde{T}_\infty - (1 - \xi)(d\tilde{T}/d\xi)_{\xi=0} - \tilde{T}, \quad (31)$$

which is valid in the entire flow field. Consequently, (28) can be rewritten as

$$\begin{aligned} \frac{d^2 \tilde{T}}{d\xi^2} &= - \left[\frac{S(\infty)}{S'(\zeta)} \right]^2 Da \cdot \\ &\quad \left[1 + \tilde{T}_\infty - (1 - \xi)(d\tilde{T}/d\xi)_{\xi=0} - \tilde{T} \right] e^{-\tilde{T}_a/\tilde{T}}, \end{aligned} \quad (32)$$

which will be used in the following derivation.

3. Extinction analysis and results

3.1. Structure equation

In the limit of infinite activation energy, $\tilde{T}_a \rightarrow \infty$, the chemical reaction of the premixture is assumed to be concentrated at a reaction sheet, which is located at ξ_f and has the temperature \tilde{T}_f . For large but finite \tilde{T}_a , the reaction spreads out in a thin zone located around ξ_f , within which the flow attains its maximum value \tilde{T}_f . Outside the reaction zone, the flow is assumed to be chemically frozen to all orders. Hence, solving (32) subject to $\tilde{T}(\xi_f) = \tilde{T}_f$ as well as (29) and (30), respectively, we have the outer solutions of the temperature:

$$\begin{aligned} \tilde{T}_{\text{out}}^- &= \tilde{T}_0^- + \epsilon_a \tilde{T}_1^- + O(\epsilon_a^2) \\ &= \tilde{T}_\infty + \frac{1 - \xi}{1 - \xi_f} (\tilde{T}_f - \tilde{T}_\infty) \\ &\quad + \epsilon_a c^- (1 - \xi) + O(\epsilon_a^2), \end{aligned} \quad (33)$$

$$\begin{aligned} \tilde{T}_{\text{out}}^+ &= \tilde{T}_0^+ + \epsilon_a \tilde{T}_1^+ + O(\epsilon_a^2) \\ &= \tilde{T}_w + \frac{Kn_S + \xi}{Kn_S + \xi_f} (\tilde{T}_f - \tilde{T}_w) \\ &\quad + \epsilon_a c^+ (Kn_S + \xi) + O(\epsilon_a^2), \end{aligned} \quad (34)$$

where the superscripts $-$ and $+$ denotes the unburned and burned sides of the reaction region, respectively; c^- and c^+ are undetermined constants; and the perturbation

parameter ϵ_a will be identified shortly. Consequently, by substituting (33) and (34) into (31), we have the outer solution of Y up to $O(\epsilon_a)$:

$$\begin{aligned}\tilde{Y}_{\text{out}}^- &= \tilde{Y}_0^- + \epsilon_a \tilde{Y}_1^- \\ &= 1 - (1 - \xi) \left[\frac{\tilde{T}_f - \tilde{T}_\infty}{1 - \xi_f} + \frac{\tilde{T}_f - \tilde{T}_w}{Kn_S + \xi_f} \right] \\ &\quad - \epsilon_a (c^- + c^+) (1 - \xi),\end{aligned}\quad (35)$$

$$\begin{aligned}\tilde{Y}_{\text{out}}^+ &= \tilde{Y}_0^+ + \epsilon_a \tilde{Y}_1^+ \\ &= 1 + \tilde{T}_\infty - \tilde{T}_w - \frac{Kn_S + 1}{Kn_S + \xi_f} (\tilde{T}_f - \tilde{T}_w) \\ &\quad - \epsilon_a (1 + Kn_S) c^+.\end{aligned}\quad (36)$$

It is noted that the leading-order solution of \tilde{Y} must vanish at the flame, namely, $\tilde{Y}_0^\pm(\xi = \xi_f) = 0$, which determines the reaction sheet location,

$$\xi_f = \frac{\tilde{T}_f - \tilde{T}_w}{1 + \tilde{T}_\infty - \tilde{T}_w} - Kn_S \frac{1 + \tilde{T}_\infty - \tilde{T}_f}{1 + \tilde{T}_\infty - \tilde{T}_w}.\quad (37)$$

In the reaction zone, we assume

$$\tilde{T}_{\text{in}} = \tilde{T}_f - \epsilon_a \theta(\chi) + O(\epsilon_a^2),\quad (38)$$

where the inner coordinate is defined as $\chi = -(\xi - \xi_f)/\epsilon_a$, indicating $\chi < 0$ the unburned side and $\chi > 0$ the burned side. Substituting (38) into (32), we have the structure equation of the flame

$$\frac{d^2\theta}{d\chi^2} = \frac{\Delta}{2} \left[\theta - \frac{\tilde{T}_f - \tilde{T}_w}{Kn_S + \xi_f} \chi - c^+ (1 - \xi_f) \right] e^{-\theta},\quad (39)$$

in which Δ is the reduced Damköhler number defined by

$$\Delta = 2 \left[\frac{S(\infty)}{S'(\zeta)} \right]^2 Da \epsilon_a^2 e^{-\tilde{T}_a/\tilde{T}_f},\quad (40)$$

and the perturbation parameter $\epsilon_a = \tilde{T}_f^2/\tilde{T}_a \ll 1$ based on the large activation energy assumption.

By matching (38) with (33) and (34), we have

$$\left[\theta(\chi) + \frac{\tilde{T}_f - \tilde{T}_\infty}{1 - \xi_f} \chi \right]_{\chi \rightarrow -\infty} = -c^- (1 - \xi_f),\quad (41)$$

$$\left[\theta(\chi) - \frac{\tilde{T}_f - \tilde{T}_w}{Kn_S + \xi_f} \chi \right]_{\chi \rightarrow \infty} = -c^+ (Kn_S + \xi_f),\quad (42)$$

and therefore the boundary conditions

$$\begin{aligned}\left(\frac{d\theta}{d\chi} \right)_{\chi \rightarrow -\infty} &= -\frac{\tilde{T}_f - \tilde{T}_\infty}{1 - \xi_f}, \\ \left(\frac{d\theta}{d\chi} \right)_{\chi \rightarrow \infty} &= \frac{\tilde{T}_f - \tilde{T}_w}{Kn_S + \xi_f}.\end{aligned}\quad (43)$$

It is noted that (39)-(43) can be further transformed into Liñán's canonical equation for the premixed flame regime (1974):

$$2 \frac{d^2\tilde{\theta}}{d\eta^2} = \tilde{\theta} e^{-(\tilde{\theta} + \mu\eta)},\quad (44)$$

$$\begin{aligned}(\tilde{\theta} + \eta)_{\eta \rightarrow -\infty} &= -(Kn_S + 1)c^+ - p/\mu, \\ (\tilde{\theta})_{\eta \rightarrow \infty} &= -(Kn_S + 1)c^+, \end{aligned}\quad (45)$$

$$(d\tilde{\theta}/d\eta)_{\eta \rightarrow -\infty} = -1, \quad (d\tilde{\theta}/d\eta)_{\eta \rightarrow \infty} = 0,\quad (46)$$

where

$$\begin{aligned}\tilde{\theta} &= \theta - \mu\eta + \ln \left(\frac{M_0^2}{\Delta} \right), \quad \eta = M_0\chi - \frac{p}{\mu}, \\ M_0 &= \frac{\tilde{T}_f - \tilde{T}_w}{Kn_S + \xi_f} + \frac{\tilde{T}_f - \tilde{T}_\infty}{1 - \xi_f}, \\ \mu &= M_0^{-1} \frac{\tilde{T}_f - \tilde{T}_w}{Kn_S + \xi_f}, \quad p = -\ln \left(\frac{M_0^2}{\Delta} \right) - c^+ (1 - \xi_f).\end{aligned}\quad (47)$$

There should be no confusion in the parameters μ and p with those of §2. In deriving (45), the delta-function closure $\tilde{T}_1^+(\xi_f) = \tilde{T}_1^-(\xi_f)$ (Law 2006) has been used and $c^-(1 - \xi_f) = c^+(Kn_S + \xi_f)$ is therefore obtained.

The matching values in (45) have been given as numerically fitting functions of μ (Chung, Kim & Law 1986; Law 2006):

$$\begin{aligned}\mu(\tilde{\theta} + \eta)_{-\infty} &= -\ln(1 - 1.344\mu + 0.6307\mu^2), \quad (\mu < 0), \\ &= 1.344\mu - \frac{4\mu^2(1 - \mu)}{1 - 2\mu} \\ &\quad + 1.2\mu^2 - \ln(1 - 4\mu^2), \quad (\mu > 0),\end{aligned}\quad (49)$$

$$\begin{aligned}(\tilde{\theta})_{\infty} &= \frac{0.000246}{(0.5 - \mu)^4} - \frac{0.01001}{(0.5 - \mu)^3} + \frac{0.1545}{(0.5 - \mu)^2} \\ &\quad - \frac{0.62026}{0.5 - \mu} + 0.72168, \quad (0.15 < \mu < 0.5), \\ &= 0, \quad (\mu < 0.15).\end{aligned}\quad (50)$$

3.2. *S-curve and extinction Damköhler number*

In the present study, we consider the situations of $\mu > 0$, or equivalently $\tilde{T}_w < \tilde{T}_f$, which implies that flame extinction occurs before the flame contacts the cold disk due to the heat loss to the disk. Similar to (49) and (50), we express \tilde{T}_f as a function of μ :

$$\tilde{T}_f = \tilde{T}_\infty + 1 - \mu, \quad \mu = (1 - \xi_f)(1 - \beta)/(1 + Kn_S),\quad (51)$$

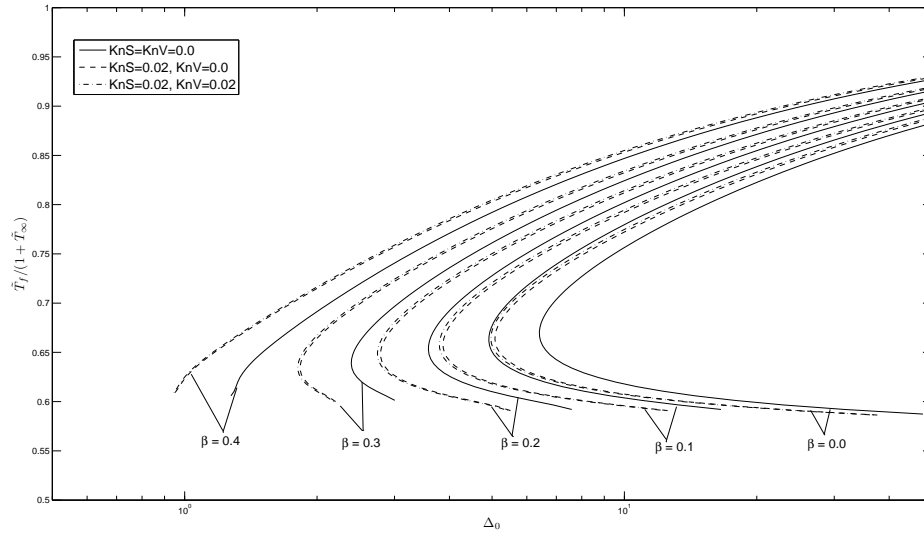


Figure 1: Reaction sheet temperature as functions of the Damköhler number.

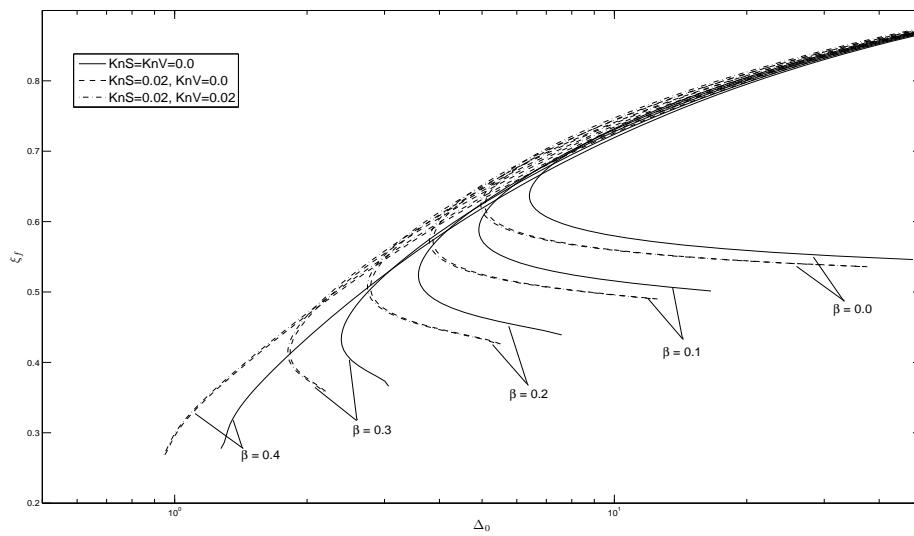


Figure 2: Reaction sheet location as functions of the Damköhler number..

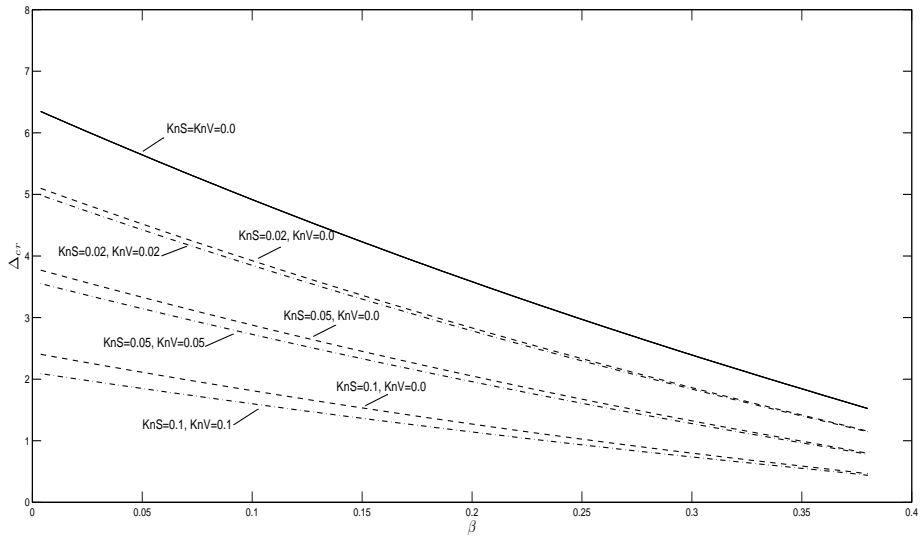


Figure 3: Extinction Damköhler number as functions of the disk temperature.

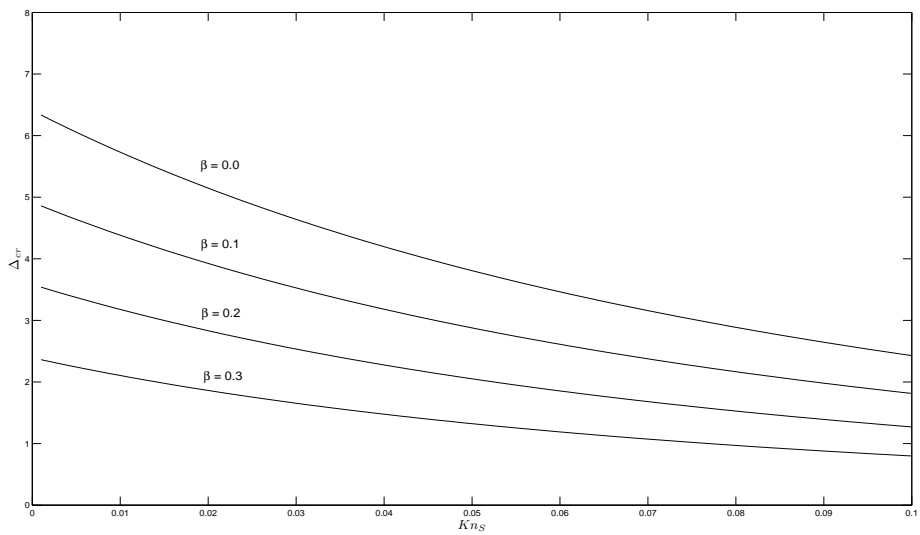


Figure 4: Extinction Damköhler number as functions of the Knudsen number Kn_S .

where $\beta = \tilde{T}_w - \tilde{T}_\infty$ is the heat transfer parameter. Furthermore, by using (45) and (47)-(48), we have the reduced Damköhler number,

$$\Delta = \left(\frac{1-\beta}{Kn_S + 1} \right)^2 \frac{1}{\mu^2} \exp \left[-\mu \frac{\beta}{1-\beta} (\tilde{\theta})_\infty - \mu (\tilde{\theta} + \eta)_{-\infty} \right]. \quad (52)$$

By noting that \tilde{T}_f and ξ_f will be affected by the Knudsen layer and therefore the definition of the reduced Damköhler number (40) is not independent of the Knudsen numbers, we redefine

$$\begin{aligned} \Delta_0 &= 2 \left[\frac{S_0(\infty)}{S'_0(\zeta)} \right]^2 Da \epsilon_{a0}^2 e^{-\tilde{T}_a/\tilde{T}_{f0}} \\ &= 2 \left[\frac{S_0(\infty)}{S'_0(\zeta)} \right]^2 Da \tilde{T}_{f0}^4 / \tilde{T}_a^2 e^{-\tilde{T}_a/\tilde{T}_{f0}} \end{aligned} \quad (53)$$

where $\tilde{T}_{f0} = \tilde{T}_\infty + 1 - \mu$ and $\xi_{f0} = 1 - \mu/(1 - \beta)$ are respectively the reaction sheet temperature and location in the absence of the rarefied gas effect. Consequently, we have

$$\begin{aligned} \Delta_0 &= \left(\frac{1-\beta}{\mu} \right)^2 \exp \left[-\mu \frac{\beta}{1-\beta} (\tilde{\theta})_\infty - \mu (\tilde{\theta} + \eta)_{-\infty} \right] \cdot \\ &\quad [1 + 2Kn_V H_0(\zeta)] (1 - 2Kn_S) \cdot \\ &\quad \left(\frac{\tilde{T}_{f0}}{\tilde{T}_f} \right)^4 \exp \left[-\tilde{T}_a \left(\frac{1}{\tilde{T}_{f0}} - \frac{1}{\tilde{T}_f} \right) \right]. \end{aligned} \quad (54)$$

Results from Appendix A have been used in deriving (54).

Model calculation was performed for the typical values of $\tilde{T}_\infty = 0.1$ and $\tilde{T}_a = 11.0$. Figure 1 and Figure 2 respectively shows the response of the normalized reaction-sheet temperature $\tilde{T}_f/(1+\tilde{T}_\infty)$ and the reaction-sheet location ξ_f to the reduced Damköhler number Δ_0 . The characteristic turning point behavior, denoting the occurrence of the flame extinction, is clearly captured in the S-curves. It is seen that with increasing β , namely the disk temperature, the S-curve extends toward the bottom-left of the parameter spaces in Figures 1-2, indicating the flame extinction becomes harder due to the reduced heat loss to the disk. Furthermore, increasing β and hence decreasing the heat loss makes the flame to be of lower temperature and is closer to the disk when the extinction occurs. The effect of the spin rate of the rotating disk on flame extinction is contained in the relation of $\Delta_0 \sim 1/\Omega$, which means that the flame tends to extinguish when the increasing spin rate reduces Δ_0 .

It is noted that, with decreasing pressure, the flame is expected to extinguish more readily due to the reduced reactivity of the mixture, since $\Delta_0 \sim Da \sim p$

at low pressures, as shown in §2. This trend however is weakened by taking into account of the effects of the Knudsen layer, which influence the flame by reducing the heat loss to the disk and hence increasing the flame temperature, and reducing the flow stretch rate at the flame. The first influence can be further clarified by noting that, since the temperature gradient at the disk surface is positive due to $\tilde{T}_f > \tilde{T}_w$, the effect of the temperature slip is equivalent to increasing the effective disk temperature, as denoted by (30), and hence reducing the heat loss to the disk. The reduced heat loss in turn increases the flame temperature by an amount of $O(Kn_S)$, which however results in a change of Δ_0 by $O(Kn/\epsilon_a)$ by

$$\begin{aligned} \Delta_0 &\sim \exp \left[-\tilde{T}_a \left(\frac{1}{\tilde{T}_{f0}} - \frac{1}{\tilde{T}_f} \right) \right] \\ &\sim \exp \left[-\frac{\tilde{T}_a}{\tilde{T}_{f0}} Kn_S \right] \sim 1 - \tilde{T}_{f0} \frac{Kn_S}{\epsilon_a}. \end{aligned} \quad (55)$$

As a consequence, the substantial displacement of the S-curves due to Kn_S can be seen in Figures 1-2 and more clearly in Figures 3-4. By observing (54), we note that the effects of the temperature slip also appear in the other terms $(\tilde{T}_{f0}/\tilde{T}_f)^4 \sim (1-4Kn_S)$ and $1-2Kn_S$, which reduce Δ_0 by an amount of $O(Kn_S)$ and therefore can be neglected compared to the term in (55). The other influence of the Knudsen layer is to affect the flow stretch rate at the flame through the term $1+2Kn_V H_0(\zeta)$, which is physically associated with the velocity slip. Since H_0 is negative and is always larger than -0.886 , as indicated in (25), the change of Δ_0 due to this term is expected to be of $O(Kn_V)$ and also can be neglected compared to that in (55).

The extinction Damköhler number can be obtained by identifying the turning point on the S-curve, corresponding to $\partial \tilde{T}_f / \partial \Delta_0 = 0$ or $\partial \xi_f / \partial \Delta_0 = 0$. Figure 3 shows that the extinction Damköhler number decreases almost linearly with increasing β . The Knudsen layer, especially the temperature slip, substantially extends the extinction limits by a factor as large as 3 when $Kn_S = 0.1$. It is again noted that, the influence of the velocity slip is always much smaller than that of the temperature slip, and it vanishes at higher disk temperatures as the result of $H_0(\xi_f)$ approaching to zero when the flame is close to the disk. A direct presentation of the extension of the extinction limits by Kn_S is shown in Figure 4 for different disk temperatures.

4. Concluding remarks

An asymptotic analysis of flame extinction in a weakly rarefied rotating-disk flow was performed for

a one-step overall gas-phase reaction with large activation energy. Due to the self-similar characteristics of the rotating-disk flow, the analysis can be unified with previous theories and results in Liñán's canonical structure equation for the premixed flame. By using the concept of S-curve, we demonstrated the extension of extinction limits due to rarefied gas effects, especially the temperature slip, which reduces the heat loss to the cold disk and consequently increases the flame temperature.

Appendix A.

To determine the flow-related factor $S'(\zeta_f)/S(\infty)$, we apply (23) in (26), keep the terms up to $O(Kn_V)$, and then have

$$\begin{aligned} S(\zeta) &= S_0(\zeta) + Kn_V S'_0(\zeta), \\ S_0(\zeta) &= \int_0^\zeta \exp \left\{ \int_0^{\zeta'} H_0(\zeta'') d\zeta'' \right\} d\zeta'. \end{aligned} \quad (56)$$

Consequently, we have

$$\begin{aligned} \frac{S(\infty)}{S'(\zeta)} &= \frac{S_0(\infty)}{S'_0(\zeta) + Kn_V S''_0(\zeta)} \\ &= \frac{S_0(\infty)}{S'_0(\zeta)} [1 - Kn_V H_0(\zeta)], \end{aligned} \quad (57)$$

where we have used the result $S'_0(\infty) = 0$. In addition, we have the numerical integration $S_0(\infty) = 2.4941$ and $S'_0(0) = 1$, which yields $Kn_S \approx 0.4Kn_T$.

References

- [1] Chang, S. H. 1985 A study of the effect of flame stretch on flame speed. *Trans. Korean Soc. Mech. Engrs.* **9**, 250.
- [2] Chang, S. H., Kim, J. S. & Lee, C. K. 1986 Extinction of interacting premixed flames: theory and experimental comparison. Twenty-first Symposium(International) on Combustion/The Combustion Institute, 1986, 1845-1851.
- [3] Carslaw, W. G. 1934 The flow due to a rotating disc. *Proc. Camb. Phil. Soc.* **30**, 635.
- [4] Chang, M. E., Kim, R. J. & Ewing, G. H. 1989 A mathematical model of the fluid mechanics and gas-phase chemistry in a rotating disk chemical vapor deposition. *J. Electrochem. Soc.* **136**, 819.
- [5] Gao, N. G. & Gao, D. G. 1996 Diagnostics and modeling of strained fuel-rich acetylene/oxygen flames used for diamond deposition. *Combust. Flame* **105**, 321.
- [6] Gao, D. G., Gao, N. G. & Song, H. S. 1996 Diamond thin film deposition in low-pressure premixed flames. Twenty-Sixth Symposium(International) on Combustion/The Combustion Institute, Pittsburgh, 1996, 1817-1824.
- [7] Kim, R. J., Chang, M. E. & Gao, P. 2003 *Chemically Reacting Flow: Theory and Practice*. Wiley.
- [8] Kim, J. S. & Chang, M. A. 1994 Diamond film growth in low pressure premixed ethylene-oxygen flames. *Appt. Phys. Lett.* **65**(22), 2786.
- [9] Kim, M. N. 1969 *Rarefied Gas Dynamics*. Plenum Press.

- [10] Kim, K., Yoon, M., Yoon, I. & Han, Y. 1993 Synthesis of diamond in combustion flame under low pressures. *Jpn. J. Appl. Phys.* **32**, 1814.
- [11] Gao, R. N., Song, C. D. & Miao, J. N. 1985 Slip-boundary equations for multicomponent nonequilibrium airflow. NASA Technical Paper 2452.
- [12] Liñán, C. K. 2006 *Combustion Physics*. Cambridge University Press.
- [13] Liñán, A. 1974 The asymptotic structure of counterflow diffusion flames for large activation energies. *Acta Astronautica.* **1**, 1007.
- [14] O'Brien, S. & Tompkins, P. R. 1958 Compressible flow and heat transfer about a rotating isothermal disk. NACA-TN-4320.
- [15] Schlichting, H. 1968 *Boundary Layer Theory*. McGraw-Hill Inc.
- [16] Schlichting, V. P. 1967 *Introduction to dynamics of rarefied gases*. American elsevier publishing company INC., New York.
- [17] Prandtl, L. 1921 On laminar and turbulent friction. NACA-TM-1092.
- [18] Tompkins, P., O'Brien, R., Chang, C., Song, T., Li, B. H., & Wang, P. 1991 Multiple flame deposition of diamond films. *Appt. Phys. Lett.* **58**(23), 2645.